© 2021. Published by The Company of Biologists Ltd | Journal of Experimental Biology (2021) 224, jeb242153. doi:10.1242/jeb.242153

RESEARCH ARTICLE

Molecular changes associated with migratory departure from wintering areas in obligate songbird migrants

Aakansha Sharma[1], Devraj Singh[1], Priya Gupta[2], Sanjay Kumar Bhardwaj[3], Inderjeet Kaur[2,4] and Vinod Kumar[1,*]

ABSTRACT

Day length regulates the development of spring migratory and subsequent reproductive phenotypes in avian migrants. This study used molecular approaches, and compared mRNA and proteome-wide expression in captive redheaded buntings that were photostimulated under long-day (LD) conditions for 4 days (early stimulated, LD-eS) or for ∼3 weeks until each bird had shown 4 successive nights of Zugunruhe (stimulated, LD-S); controls were maintained under short days. After ∼3 weeks of LD, photostimulated indices of the migratory preparedness (fattening, weight gain and Zugunruhe) were paralleled with upregulated expression of *acc*, *dgat2* and *apoa1* genes in the liver, and of *cd36*, *fabp3* and *cpt1* genes in the flight muscle, suggesting enhanced fatty acid (FA) synthesis and transport in the LD-S state. Concurrently, elevated expression of genes involved in the calcium ion signalling and transport (*camk1* and *atp2a2*; *camk2a* in LD-eS), cellular stress (*hspa8* and *sod1*, not *nos2*) and metabolic pathways (*apoa1* and *sirt1*), but not of genes associated with migratory behaviour (*adcyap1* and *vps13a*), were found in the mediobasal hypothalamus (MBH). Further, MBH-specific quantitative proteomics revealed that out of 503 annotated proteins, 28 were differentially expressed (LD-eS versus LD-S: 21 up-regulated and 7 down-regulated) and they enriched five physiological pathways that are associated with FA transport and metabolism. These first comprehensive results on gene and protein expression suggest that changes in molecular correlates of FA transport and metabolism may aid the decision for migratory departure from wintering areas in obligate songbird migrants.

KEY WORDS: Bunting, Gene expression, Migration, Proteome, Songbird

INTRODUCTION

Twice a year, billions of birds undertake to-and-fro long-distance nocturnal journeys between breeding grounds in the north and wintering grounds in the south. Day length regulates these predictable seasonal migratory movements and the subsequent reproductive state in avian migrants (Ramenofsky and Wingfield, 2007; Rani et al., 2017). In particular, increasing photoperiod induces the development of spring migratory and subsequent reproductive phenotypes in avian migrants. This is faithfully reproduced under laboratory conditions. For instance, when exposed to appropriate photoperiods, captive birds exhibit a migratory phenotype (body fattening and weight gain, and intense nocturnal activity – the Zugunruhe used as a proxy for the propensity of birds to migrate; Berthold and Querner, 1988) and gonadal maturation, used as a proxy for reproduction (Lofts, 1975). Several lines of evidence suggest the mediobasal hypothalamus (MBH) as the key brain area for the photoperiodic induction. The MBH contains receptors and signal transduction molecules for photoperiod perception and phototransduction, a time-keeping mechanism to assess the photoperiod change, and effector (output) pathways that convert the photoperiodic message into a biological response (Surbhi and Kumar, 2014; Cassone and Yoshimura, 2015; Kumar and Mishra, 2018). It is therefore the site for controlling the photoperiodic induction of multiple processes, including the photostimulated development of spring migratory and reproductive phenotypes in migratory songbirds (Sharp, 2005; Yoshimura, 2006; Nakao et al., 2008; Rastogi et al., 2011; 2013; Stevenson and Kumar, 2017).

Both field and controlled laboratory studies demonstrate that migratory preparedness is linked to fat accumulation and changes in the activity of enzymes associated with metabolism (Odum, 1960; Newton, 2008; Weber, 2009). In fact, the association of accumulated fat stores and enzyme activity with departure decision from stopover sites has been reported in several songbird migrants (Bairlein, 1985; Ramenofsky, 1990; Fusani et al., 2013; Lupi et al., 2016). In particular, changes in fatty acid (FA) synthesis (lipogenesis) in the liver and its transport to skeletal (flight) muscles serve as reliable indices for readiness for the departure and subsequent prolonged nocturnal flights in migratory songbirds (McFarlan et al., 2009; Banerjee and Chaturvedi, 2016).

A key question is whether the information about peripheral fat accumulation is integrated into the photoperiodic control mechanism(s) in the MBH. To address this, we compared gene and protein expression in migratory redheaded buntings (*Emberiza bruniceps*) that were long-day (LD) photostimulated for 4 days (early stimulated: LD-eS) or ∼3 weeks (stimulated: LD-S), and with that in birds maintained under non-stimulatory short-day (SD) conditions. Buntings are a Palearctic-Indian obligate migrant songbird with predictable yearly migrations between breeding and wintering areas (Ali and Ripley, 1999) and exhibit a spring migratory phenotype and testicular maturation under LD (Sharma et al., 2018a).

Here, we first examined the expression of genes coding for enzymes involved in FA synthesis (acetyl CoA carboxylase, *acc*; FA synthase, *fasn*; diacylglycerol *O*-acyltransferase 2, *dgat2*) in the liver, and those coding for proteins/enzymes involved in FA transport in both liver (apolipoprotein 1, *apoa1*) and flight muscles (FA translocase, *cd36*/*fat*; FA binding protein 3, *fabp3*; carnitine palmitoyltransferase1, *cpt1*). This was done to show changes in the transcription of genes associated with FA synthesis and transport

[1]Department of Zoology, University of Delhi, Delhi 110 007, India. [2]International Centre for Genetic Engineering and Biotechnology, Aruna Asaf Ali Marg, Delhi 110 067, India. [3]Department of Zoology, CCS University, Meerut 250 004, India. [4]Department of Biotechnology, Central University of Haryana, Mahendergarh, Haryana 123031, India.

*Author for correspondence (drvkumar11@yahoo.com)

A.S., 0000-0001-6838-0060; D.S., 0000-0002-1202-9826; P.G., 0000-0001-6192-7051; S.K.B., 0000-0002-3847-2607; I.K., 0000-0001-8778-1396; V.K., 0000-0002-0523-8689

Received 17 December 2020; Accepted 28 April 2021

Journal of Experimental Biology (2021) 224, jeb242153. doi:10.1242/jeb.242153

with the photoperiod-induced transition of buntings into the migratory state, based on a previous study in which these genes were found to be upregulated in expression in both liver and muscle during the photostimulated state (Sharma and Kumar, 2019).

Then, we measured the expression of genes associated with a few key physiological pathways in the MBH that might show alteration with the photoperiodic induction of the migratory state (Boss et al., 2016; Sharma et al., 2018a,b). We chose candidate genes associated with neural processes, cellular stress, metabolic status and migratory behaviour in view of the role of photoperiod in controlling multiple processes at the brain level (Sharp, 2005; Nakao et al., 2008; Rastogi et al., 2013; Cassone and Yoshimura, 2015; Stevenson and Kumar, 2017). For example, the activation of the Ca^{2+}-signalling and transport pathway (*camk1* and *camk2a*, encoding calcium/calmodulin-dependent protein kinase 1 and II alpha; and *atp2a2*, encoding ATPase sarcoplasmic Ca^{2+} transporting 2 protein) has been reported in photostimulated migratory willow warblers (*Phylloscopus trochilus*; Boss et al., 2016) and blackheaded buntings (*Emberiza melanocephala*; Sharma et al., 2018a,b). Although not shown in birds, the alteration in Ca^{2+}-signalling has been reported to correlate with key neural processes in some animals; for example, the neurogenesis and maintenance of synaptic connections (Berridge et al., 2000; Bouron, 2020). Additionally, there is evidence for neurogenesis and neuronal recruitment in different brain regions during the migratory season in avian migrants, such as white-crowned sparrows (*Zonotrichia leucophrys gambelii*; LaDage et al., 2011) and migratory reed warblers (*Acrocephalus scirpaceus*; Barkan et al., 2014). Increased neuronal activity and neurogenesis may indicate an enhanced capacity for the integration of sensory inputs and the ability to use acquired information for migration and navigation (Åkesson and Hedenström, 2007; Muheim et al., 2006; Warren et al., 2010). It is, therefore, likely that genes associated with Ca^{2+} signalling and transport serve as important molecular correlates of enhanced hypothalamic activity during the photostimulated state.

Further, we reasoned that changes in metabolic status and oxidative stress as a consequence of heightened activity during the photostimulated state would be reflected at the brain level. To test this, we measured *hspa8* (a member of heat shock protein family), *sod1* (encoding superoxide dismutase) and *nos2* (encoding inducible nitric oxide synthase, iNOS) expression to show the effects on the cellular oxidative stress (Jones et al., 2008; Raja-Aho et al., 2012; Sharma et al., 2018b; Valek et al., 2019). Concurrently, we measured *apoa1* (encoding apolipoprotein A1) and *sirt1* (encoding sirtuin 1) expression, levels of which correspond to migratory fattening and serve as indices of the metabolic status (energy reserve) in songbird migrants (Trivedi et al., 2014; Frias-Soler et al., 2020). In addition, we measured *adcyap1* (encoding pituitary adenylate cyclase activating polypeptide, PACAP) and *vps13a* (encoding vacuolar protein sorting-associated protein 13A) expression. PACAP is light sensitive, and is involved in circadian clock phase shifts (Harrington et al., 1999; Nowak and Zawilska, 2003); hence, the change in *adcyap1* gene expression, if any, could be associated with circadian clock-controlled physiological and behavioural shifts that occur with photoperiodic induction of the migratory phenotype in migratory songbirds including buntings (Bartell and Gwinner, 2005; Rani et al., 2006; Singh et al., 2015). There is also a reported association of the allele size of the *adcyap1* gene with Zugunruhe as well as with migratory distance in migratory blackcaps (*Sylvia atricapilla*; Mueller et al., 2011). Likewise, *vps13a* gene expression has been linked with migration directionality in *Vermivora* warblers (Toews et al., 2019).

Finally, we sought to examine changes at the proteome level rather than at the more commonly used transcriptome level, as it can reveal the complex hypothalamic processes involved in migratory preparedness and subsequent gonadal maturation. For this, we used a MBH-specific proteome-wide assay, and identified key proteins that were differentially expressed with the photostimulated transition from the LD-eS to the LD-S state. We used a mass spectrometry-based quantitative proteome approach that facilitates protein profiling and assessment of protein interactions involved in biological processes (Yugandhan et al., 2019).

MATERIALS AND METHODS

Animal maintenance

All procedures were approved and carried out in accordance with guidelines of the Institutional Animal Ethics Committee (IAEC) of Department of Zoology, University of Delhi, India (Institutional Ethical Approval number: DU/ZOOL/IAEC-R/2015/04). This study was done on adult male redheaded buntings (*Emberiza bruniceps* Brandt 1841), which were procured from an overwintering flock in late February, and acclimated to captive conditions for ca. 2 weeks in an outdoor aviary (3×2.5×2.5 m) under the natural photoperiod (~11.3 h, sunrise to sunset) and temperature (21–25°C) conditions. The birds were then brought indoors and maintained under SD conditions (8 h light and 16 h dark), and were singly housed in activity cages (42×30×52 cm; one bird per cage) placed in independent photoperiodic boxes (70×50×70 cm; one cage per photoperiodic box) for a period of 4 weeks, until the experiment began. Each cage was equipped with two perches and mounted with a passive infrared (PIR) motion sensor (DSC, LC100 PI digital PIR detector, Concord, ON, Canada) to monitor the activity of the bird inside the cage. Photoperiodic boxes were lit by compact fluorescent lamps (CFL, Phillips) providing a light period of 300 lx and a dark period of <1 lx. HOBO temperature loggers monitored 24 h temperature of each box, and this was maintained over 24 h at 24.7±0.07°C (mean±s.e.m.). All birds had *ad libitum* access to food and water, which were replenished only during the light phase. Under SD conditions, buntings maintain small testes and retain responsiveness to the stimulatory effects of long photoperiod; we called them SD-photosensitive birds.

Experiment

The experiment used a total of 21 adult male redheaded buntings maintained under SD conditions (SD photosensitive birds: body mass 21–24 g, volume of unstimulated testes 0.33–0.52 mm^3). Fig. S1 describes the experimental protocol. Briefly, 16 birds were exposed to a stimulatory 12.5 h photoperiod (12.5 h light:11.5 h dark) for 4 days (n=8; LD-eS) or until each bird had shown 4 successive nights of Zugunruhe (~3 weeks; n=8; LD-S), which was verified by the videographs recorded using the night vision camera. A 12.5 h light period per day approximated the natural daylight (sunrise to sunset) available in the wild at the time of spring migration in early April. We called birds exposed to LD conditions for 4 days 'early stimulated' based on our earlier bunting studies in which exposure to LD conditions for 1 or 2 days triggered photoperiodic induction at the molecular level in the hypothalamus (Majumdar et al., 2015; Mishra et al., 2018). The remaining 5 birds were retained for the next 3 weeks under SD conditions, and served as controls (SD state). The temperature over 24 h was maintained at 24.7±0.07°C.

Journal of Experimental Biology (2021) 224, jeb242153. doi:10.1242/jeb.242153

Monitoring of changes in behaviour and physiology

We monitored the 24 h activity–rest pattern, body mass and testis size as faithful markers of behavioural and physiological changes associated with migration and gonadal maturation (Berthold and Querner, 1988; Trivedi et al., 2014; Sharma et al., 2018a).

The activity–rest pattern over 24 h reflects circadian clock effects, which mediate the phase transition from the non-migratory to migratory state in songbirds (Bartell and Gwinner, 2005; Rani et al., 2006). Photostimulated Zugunruhe (nocturnal migratory restlessness) also reflects faithfully the temporal pattern of actual migration in the wild (Gwinner, 1972). The activity of each bird was recorded by a PIR motion sensor mounted in front of the activity cage. The PIR sensor detected and recorded general movements including perch hopping activity of the bird in its cage, and transferred and stored these in 5 min bins into designated channels of the computerized data acquisition system. The collection, analysis and graphic presentation of the 24 h activity–rest pattern were done by using The Chronobiology Kit software (Stanford Software Systems). To compare the overall distribution of activity over 24 h between groups, we first averaged hourly activity for 4 consecutive days for every bird in all three groups, and then normalized the average value relative to the hour with the maximal value, which was given a score of 100 (Sharma and Kumar, 2019). The normalized individual scores were plotted in a circular polar plot using a MS-Excel based add-in application, showing the magnitude in concentric circles and the phase in radial lines for each bird.

Each bird was weighed on a top pan balance to an accuracy of 0.1 g on day 1 of the experiment (initial value) and 1 day before the bird was used for harvesting the tissue samples (final value). From these values, we calculated change in body mass (Δbody mass=final value−initial value). Further, using a subjective criterion on a 0–5 scale (see below), we also recorded subcutaneous fat accumulation in each bird 1 day before tissue harvesting in order to assess body fattening as a result of photoperiodic exposure. This scheme of fat scoring, which is routinely done in our laboratory for buntings (Malik et al., 2004; Budki et al., 2009), is based on previous studies in songbird migrants (Helms and Drury, 1960; Wingfield and Farner, 1978; Biebach et al., 1986). The scores run as follows: 0=no visible subcutaneous fat deposits, 1=light fat deposits overlying musculature (musculature remains clearly visible), 2=heavier fat deposits overlying musculature (vasculature still visible), 3=fat deposits overlying the entire region, 4=areas filled with whitish, bulging fat deposits, and 5=copious fat deposits all over three regions.

The size of the left testis was measured to an accuracy of 0.5 mm at the beginning of the experiment by laparotomy and at the end of the experiment, prior to tissue samples being taken. Laparotomy is a routine procedure carried out in our laboratory. Here, the testes were located through a small incision on the left flank between the last two ribs in birds under general anaesthesia (a mixture of ketamine/xylazine solution: 67.5 mg ketamine+7.5 mg xylazine per kg body mass). The dimensions of the left testis were measured to an accuracy of 0.5 mm, and from these, testis volume was calculated using the formula $4/3\pi ab^2$ (where a is half the length and b is half the width; Budki et al., 2009). The incision was sutured, and an antibacterial skin cream (Soframycin, Aventis Pharma Ltd) was applied. The bird was returned to its cage on to a warm pad for ∼30 min, and the resumption of normal perch hopping in ∼1 h indicated full recovery of the bird from anaesthesia effects.

Measurement of gene expression in the liver, muscle and hypothalamus

At the end of the experiment, half an hour before lights off (SD: hour 7.5 h; LD-eS and LD-S: hour 12 h; where hour 0=lights on), birds were killed by decapitation (an unanticipated, quick procedure lasting ∼10 s), which was used to preclude possible anaesthesia effects on mRNA expression (Staib-Lasarzik et al., 2014). The liver and pectoral muscle, which is a dominant avian flight muscle, and MBH were harvested. To obtain the MBH, the brain was placed with its ventral side up, and two coronal incisions were made to isolate the diencephalon; the MBH was then removed in the shape of an inverted V by placing longitudinal incisions on either side of the third ventricle (Olkowicz et al., 2016; Mishra et al., 2018). Tissues were snap-frozen on dry ice and stored at −80°C until use.

Using RT-qPCR, we measured the expression of genes associated with FA synthesis and transport in the liver (*acc*, *fasn*, *dgat2* and *apoa1*), and with FA transport in the muscle (*cd36*, *fabp3* and *cpt1*). In the MBH, we measured the expression of genes involved in calcium signalling and transport (*camk1*, *camk2a* and *atp2a2*), metabolism (*apoa1* and *sirt1*), cellular stress/energy demand (*hspa8*, *sod1* and *nos2*), and migratory behaviour (*adcyap1* and *vps13a*). These genes were chosen based on microarray, transcriptome and gene expression studies in migratory white-crowned sparrows (*Z. leucophrys gambelii*; Jones et al., 2008), willow warblers (*P. trochilus*; Boss et al., 2016), blackheaded buntings (*E. melanocephala*; Sharma et al., 2018b) and redheaded buntings (*E. bruniceps*; Sur et al., 2020).

For each gene expression assay (n=5 samples per tissue), total RNA was extracted from each sample using Trizol solution (Ambion, 15596-018), as per the manufacturer's protocol. The concentration and purity of RNA was checked by NanoDrop™ 2000C (ThermoFisher Scientific, Wilmington, DE, USA); an A_{260}/A_{280} ratio of 1.9–2.0 was considered as pure for RNA. To assess the integrity of the RNA, we proceeded with cDNA preparation and then used PCR to amplify the cDNA from each sample using primers (*beta-actin*) that generate a greater amplicon size (∼750 bp). Only those cDNA samples that could amplify *beta-actin* (∼750 bp) were used for the measurement of gene expression by qPCR (Gong et al., 2006). For reverse transcription, 1 µg pure RNA was treated with RQ1 RNase-free DNase (Promega, M610A) for 30 min at 37°C. The reaction was stopped by adding 1 µl of the stop solution (50 mmol l^{-1} EDTA) and incubating samples at 65°C for 10 min. The samples were then reverse transcribed to synthesize cDNA using Revert Aid First Strand cDNA synthesis kit (ThermoFisher Scientific, K1622) by incubation of DNase-treated RNA first with random hexamers for 5 min at 25°C, and then with 10 mmol l^{-1} dNTP mix, reverse transcriptase and RNase inhibitor enzyme for 60 min at 42°C. The product of this reaction (post-assessment of RNA integrity) was used for qPCR. Gene-specific primers were designed from gene sequences available with us (*acc*, *fasn*, *dgat2*, *cd36*, *fabp3*, *cpt1*, *atp2a2*, *sirt1*, *hspa8*, *sod1*, *nos2* and *adcyap1*; Trivedi et al., 2014; Sharma et al., 2018a,b; Sharma and Kumar, 2019; Sur et al., 2019, 2020) or from those we cloned for this study (*apoa1*, *vps13a*, *camk1* and *camk2a*). We cloned a gene sequence by using degenerate primer sequence based on a conserved region of the gene, and the amplified products (>500 bp) of bunting hypothalamus cDNA templates were commercially sequenced (Eurofins, Bangalore, India) and subjected to a NCBI database nucleotide BLAST search to ascertain gene identity. Identified gene sequences were submitted to NCBI GenBank (for the accession numbers, see Table S1). qPCR was carried out in duplicate with SYBR green chemistry and a reaction volume of 6 µl

(3 µl 1× SYBR Green, 1 µl each primer and 1 µl cDNA). We ran 2-step qPCR for 40 cycles, with each cycle lasting for 75 s (denaturation at 95°C for 15 s and annealing at 60°C for 60 s). Each PCR plate included *beta-actin* as a control (reference) gene (Sharma et al., 2018a). Consistent with guidelines for the use of qPCR (Bustin et al., 2009), relative mRNA expression was determined by the ΔΔCt method (Livak and Schmittgen, 2001), as in our previous studies on redheaded buntings (Sharma et al., 2018a). The cycle threshold (Ct) determined by fluorescence surpassing the background noise was used to calculate ΔCt (Ct[gene of interest]−Ct[reference gene]). The Ct values normalized against the Ct value of the pooled cDNA from all samples gave ΔΔCt, and the negative value of ΔΔCt powered to 2 ($2^{-\Delta\Delta Ct}$) gave the relative mRNA expression level.

Differential protein expression profiling: mass spectrometry

Mass spectrometry (LC-MS/MS) was carried out for global profiling and differential protein expression in the MBH using three samples each from LD-eS and LD-S. Each MBH sample was homogenized in protein extraction buffer (20 mmol l^{-1} Tris buffer pH 8, 8 mol l^{-1} urea, 4% w/v Chaps, 0.5% v/v Triton X-100, 10 mmol l^{-1} DTT and protease inhibitor cocktail). The lysate was centrifuged at 15,142 ***g*** at 4°C for 1 h, the supernatant collected in a fresh tube and protein concentration determined by using BCA Protein Assay Kit (ThermoFisher Scientific, 23225). An equal amount (150 µg) of total protein from each sample was reduced and alkylated using 10 mmol l^{-1} DTT for 1 h followed by treatment with 40 mmol l^{-1} iodoacetamide for 1 h at room temperature. The samples were cleaned up by acetone precipitation and the precipitated proteins were centrifuged at 15,871 ***g*** at 4°C for 1 h. The pellet was washed with ice-cold acetone and then re-suspended in 1 ml of 100 mmol l^{-1} tetraethylammonium tetrahydroborate (TEAB). Protein digestion was performed by incubating the samples overnight at 37°C with trypsin (enzyme: total protein, 1:50; Promega Corporation). The peptides thus obtained were labelled with TMTsixplex label reagent (ThermoFisher Scientific, 90061) as per the manufacturer's protocol. Briefly, 0.8 mg TMT label (brought to room temperature) was added to 41 µl of anhydrous acetonitrile, and the reagent was allowed to dissolve for 5 min with occasional vortexing. To this, a total of 100 µl of protein sample was added and incubated for 1 h at room temperature. For reaction quenching, 8 µl of 5% hydroxylamine was added to each tube and incubated for 15 min at the room temperature. TMT-labelled samples were then mixed in equal amounts in a new centrifuge tube, vacuum dried and then used for LC-MS/MS analysis. A brief outline of the procedure for protein purification is given in Fig. S1.

The prepared samples (digested and labelled peptides) were analysed using an Orbitrap Velos Pro mass spectrometer coupled with a nano-LC 1000 (ThermoFisher Scientific). For this, the peptide mixtures were loaded onto a reverse-phase C-18 pre-column (Acclaim PepMap, 75 µm×2 cm, particle size 3 µm, pore size 100 Å, ThermoFisher Scientific), in line with an analytical column (Acclaim PepMap, 50 µm×15 cm, particle size 2 µm, pore size 100 Å). The peptides were separated using a gradient of 5% to 50% of solvent B (0.1% formic acid in 95/5 acetonitrile/water). The eluted peptides were injected into the MS and spectra were acquired in the Orbitrap at a resolution of 60,000. A minimum of 1000 counts was needed to trigger the MS/MS using HCD (higher-energy collisional dissociation) and the daughter ions were recorded in the Orbitrap at a resolution of 7500. The charge-state screening of the precursor and monoisotopic precursor selection was enabled, and an unassigned charge state and singly charged ions were rejected. The acquired spectra were analysed using the SEQUEST algorithm in the Proteome Discoverer (PD, v.1.4) software, with a precursor tolerance of 20 ppm and tolerance of 0.1 Da for MS/MS against the *Ficedula albicollis* database (Fic_Alb1.5) and two missed cleavages were allowed. The resultant identified peptides were validated using Percolator at 5% false discovery rate (FDR; q-value<0.05), which uses PEP (posterior error probability) and q-value for the validation. The proteins with fold-change (LD-S/LD-eS) of <0.5 (down-regulated) or >1.5 (up-regulated) were considered to be differentially expressed. We also performed functional analysis, and annotated proteins and pathways based on GO enrichment using RefSeq protein ID, protein family identification (PFAM) and KEGG using the DAVID database (Dennis et al., 2003). A pathway with P<0.05 was considered as significantly enriched.

To decipher a functional linkage of differentially expressed proteins, we performed STRING network analysis (string-db.org, v.11.0; a database of known and predicted protein–protein interactions), with data in the background from migratory *F. albicollis*. The network was drawn based on the confidence values, i.e. the strength of the data support was based on text mining, experiments, databases, co-expression, neighbourhood and co-occurrence. Based on the nature and quality of the support evidence, each interaction was given a score between 0 (lowest) and 1 (highest). The minimum interaction score was set to a medium confidence value of 0.400. The network STRING diagram is composed of nodes (which represent proteins) and edges (which represent protein–protein interactions). Whereas filled nodes represent known or predicted 3D structure, the empty nodes represent proteins with unknown 3D structure.

Statistics

We used GraphPad Prism v.6.0 (GraphPad Software Inc., San Diego, CA, USA) for statistical analysis and data plots. One-way ANOVA was used to analyse significant differences, except for fat score data, for which we used the Kruskal–Wallis test. If these tests revealed a significant difference, we used the Newman–Keuls *post hoc* test or Dunn's *post hoc* test (for fat score only) for the group comparison. Pearson's correlation coefficient was calculated to show the relationship of genes involved in fatty acid synthesis with body mass gain, and of genes involved in the transport of fatty acids to flight muscle with *Zugunruhe*. The proteome data were analysed by the SEQUEST algorithm in PD v.1.4 software. For statistical significance, alpha was set at 0.05.

RESULTS

Photostimulated changes in behaviour and physiology

In contrast to diurnal activity patterns under SD and LD-eS, buntings under LD-S showed a transition to predominantly night-time activity (Fig. 1A; Fig. S1). This was nocturnal Zugunruhe, as confirmed by videographs (data not shown). We found a significant difference between photoinduced states ($F_{2,18}$=7.936, P=0.0034, one-way ANOVA), with night-time activity higher in the LD-S than in the SD and LD-eS states (P<0.05, Newman–Keuls *post hoc* test; Fig. 1B). Consistent with this, we also found significant differences between states in fat score (KW statistics=13.62, P=0.0001, Kruskal–Wallis test; Fig. 1C), Δbody mass ($F_{2,18}$=7.536, P=0.0042, one-way ANOVA; Fig. 1C) and testis size ($F_{2,18}$=11.67, P=0.0006, one-way ANOVA; Fig. 1D). Buntings were fatter, gained body mass and had larger testes in the LD-S than in the SD and LD-eS states (P<0.05, Newman–Keuls or Dunn's *post hoc* test).

Journal of Experimental Biology (2021) 224, jeb242153. doi:10.1242/jeb.242153

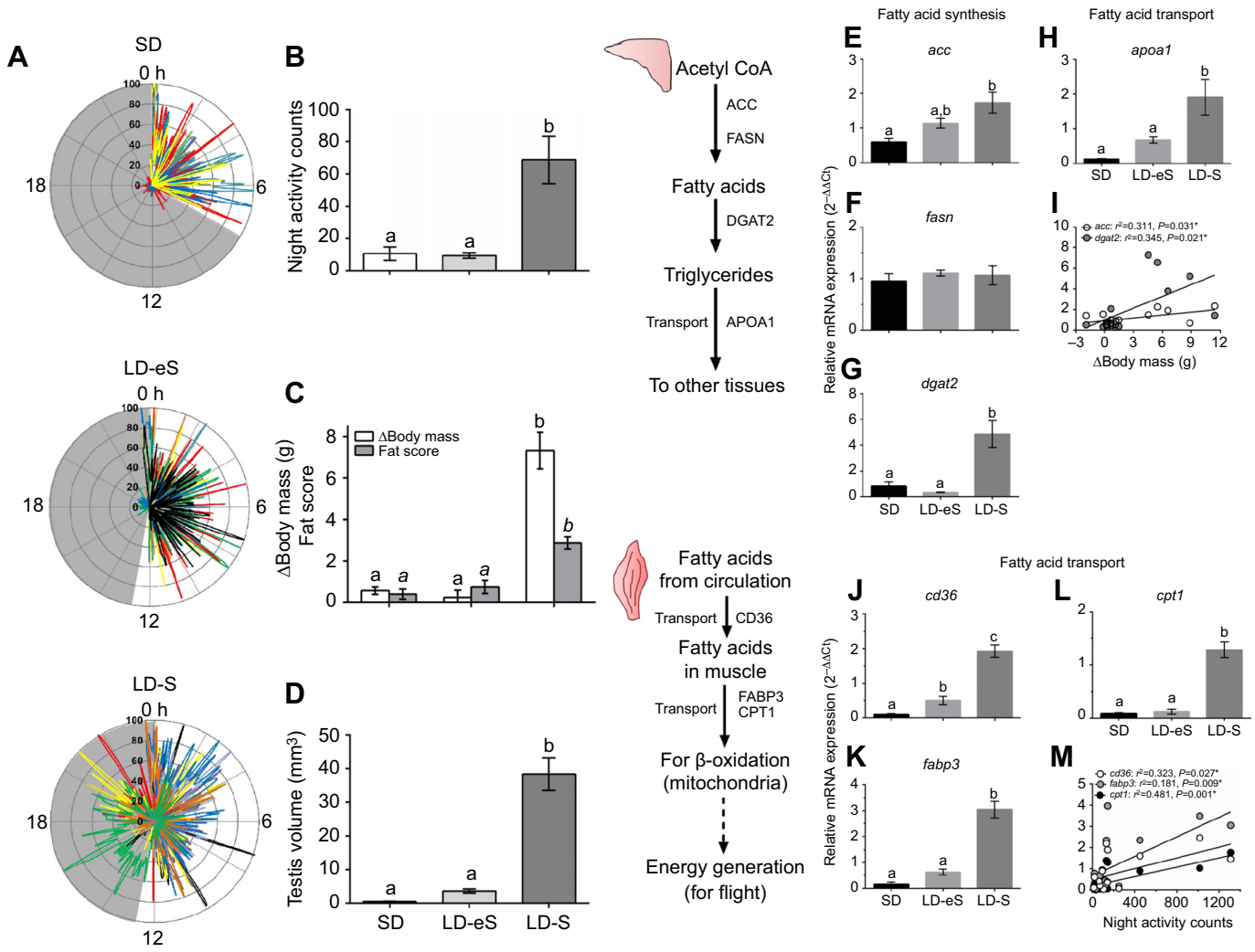

Fig. 1. Photostimulated changes in behaviour and physiology, and gene expression. (A) Polar plots of normalized activity counts over 24 h, with each line representing an individual bird, for the three different conditions: SD, short day; LD-eS, long day – early stimulated; LD-S, long day – stimulated (see Materials and Methods for details). Open and shaded areas are the light and dark periods, respectively. (B–D) Mean (±s.e.m.) night activity (Zugunruhe; B), weight gain (change in body mass) and fat score (C), and testis volume (D) in photoperiod-induced states (SD, n=5; LD-eS, n=8; LD-S, n=8). (E–H) Mean (±s.e.m.; n=5) mRNA expression of *acc* (E), *fasn* (F), *dgat2* (G) and *apoa1* (H) genes in the liver in the SD, LD-eS and LD-S states. (J–L) Mean (±s.e.m.; n=5) mRNA expression of *cd36* (J), *fabp3* (K) and *cpt1* (L) genes in flight muscles in the SD, LD-eS and LD-S states. Different letters indicate a significant difference between states (Newman–Keuls *post hoc* test following one-way ANOVA, or Dunn's *post hoc* test following Kruskal–Wallis test). (I,M) Scatter plots with Pearson's correlation coefficient (r^2-value) and significance levels (P-value) showing the relationship of *acc* and *dgat2* expression to weight gain (I) and *cd36*, *fabp3* and *cpt1* expression to night activity (M). Lines denote significant linear regression. For statistical significance, α was set at 0.05. The schematic outline in the middle illustrates functional pathways involving genes that were measured in the liver and muscle.

Gene expression supports FA synthesis in liver and its transport to flight muscles

Both hepatic and muscular gene expression supported enhanced FA synthesis and transport in the LD-S state. There was a significant difference in mRNA levels of genes associated with FA synthesis (*acc*: $F_{2,12}$=7.76, P=0.007; *dgat2*: $F_{2,12}$=15.47, P=0.0005) and transport (*apoa1*: $F_{2,12}$=9.22, P=0.004, one-way ANOVA) in the liver, with higher mRNA levels in the LD-S than in the SD and LD-eS state (not for *acc*; P<0.05, Newman–Keuls *post hoc* test; Fig. 1E–H). However, we did not find a change in *fasn* expression ($F_{2,12}$=0.331, P=0.725). There was also a positive correlation of expression of genes involved in FA synthesis (both *acc*: r=0.557, r^2=0.311, P=0.031; and *dgat2*: r=0.587, r^2=0.345, P=0.0213) mRNA levels with weight gain (Δbody mass; Fig. 1I).

Likewise, there was a significant difference in gene expression associated with FA transport (*cd36*: $F_{2,12}$=56.58, P<0.0001; *fabp3*: $F_{2,12}$=59.03, P<0.0001; *cpt1*: $F_{2,12}$=54.33, P<0.0001; one-way ANOVA) in the muscle, with significantly higher mRNA levels in the LD-S than in the SD and LD-eS state (P<0.05, Newman–Keuls *post hoc* test; Fig. 1J–L). The mRNA levels of *cd36*, in particular, were also higher in the LD-eS than in the SD state (Fig. 1J). The overall mRNA levels of *cd36*, *fabp3* and *cpt1* were positively correlated with night activity (Zugunruhe) levels (*cd36*: r=0.568, r^2=0.323, P=0.027; *fabp3*: r=0.646, r^2=0.417, P=0.0092; *cpt1*: r=0.694, r^2=0.481, P=0.0041; Fig. 1M).

Molecular changes in the MBH

Gene expression

We found significant changes in the expression of genes associated with calcium ion signalling and transport, cellular stress and metabolic status, but not with migratory behaviour. There was a significant difference in mRNA levels of both Ca^{2+}-signalling kinases (*camk1*:

Journal of Experimental Biology (2021) 224, jeb242153. doi:10.1242/jeb.242153

$F_{2,12}$=39.50, P<0.0001; *camk2a*: $F_{2,12}$=44.64, P<0.0001) and ATPase sarcoplasmic transport protein (*atp2a2*: $F_{2,12}$=13.82, P=0.0008, one-way ANOVA), but with subtle differences (Fig. 2A–C). As compared with the SD state, *camk1* mRNA levels were higher in the LD-S state and *camk2a* levels were higher in the LD-eS state, whereas *atp2a2* mRNA levels were higher in both the LD-eS and LD-S state (P<0.05, Newman–Keuls *post hoc* test; Fig. 2A–C).

Likewise, we found significant differences in the expression of genes associated with cellular and metabolic (oxidative) stress (*hspa8*: $F_{2,12}$=20.03, P=0.0002; *sod1*: $F_{2,12}$=17.82, P=0.0003; however, no difference in *nos2*: $F_{2,12}$=0.702, P=0.515; one-way ANOVA; Fig. 2D–F). The overall *hspa8* and *sod1* mRNA levels were higher in the LD-S state than in the SD and LD-eS state (P<0.05, Newman–Keuls *post hoc* test; Fig. 2D–F).

Consistent with differential energy demands, there were significant changes in the expression of genes that reflect metabolic status (*apoa1*: $F_{2,12}$=38.34, P<0.0001; *sirt1*: $F_{2,12}$=26.05, P<0.0001; one-way ANOVA). Expression of both

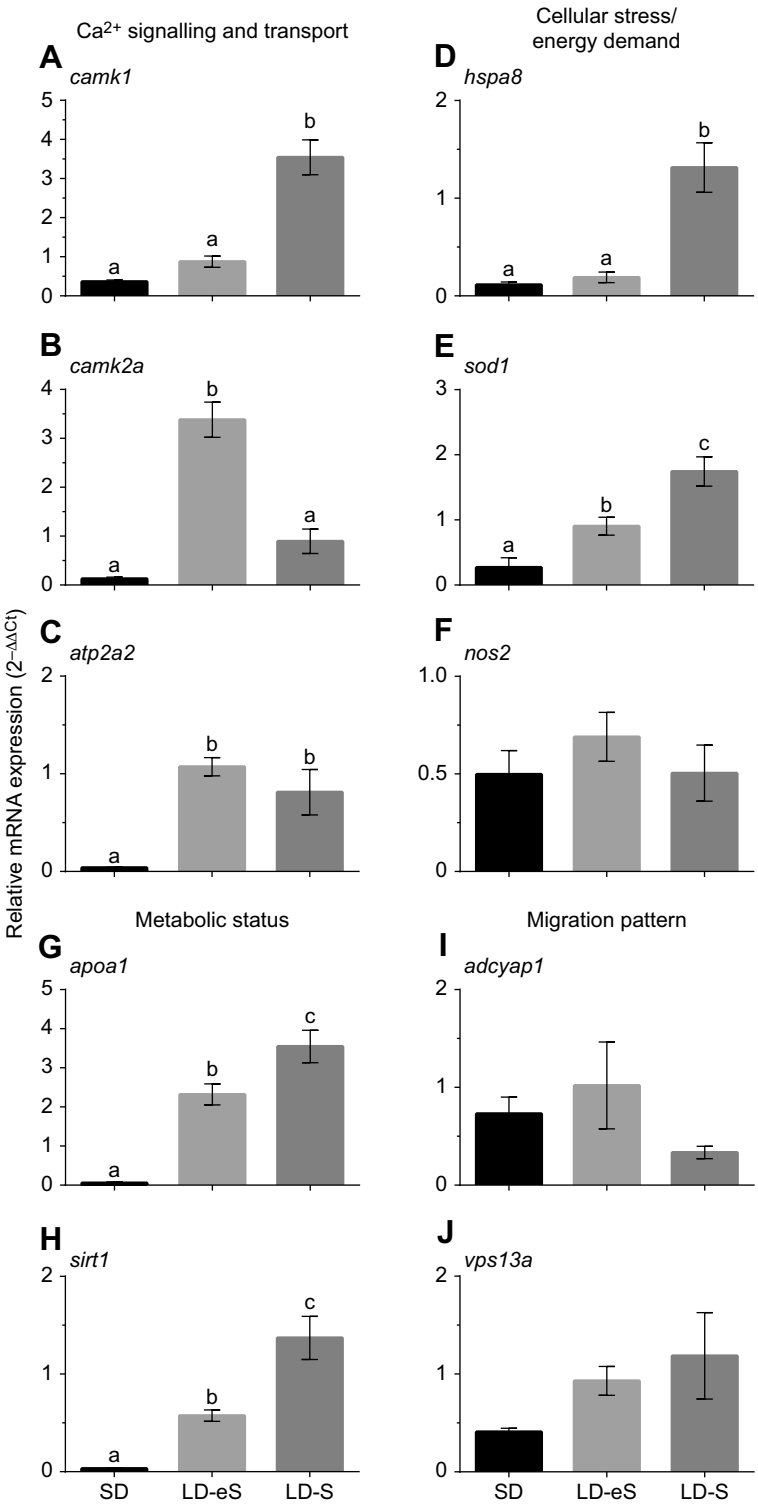

Fig. 2. Changes in hypothalamic gene expression. Mean (±s.e.m.; n=5) expression of *camk1* (A), *camk2a* (B), *atp2a2* (C), *hspa8* (D), *sod1* (E), *nos2* (F), *apoa1* (G), *sirt1* (H), *adcyap1* (I) and *vps13a* (J) under SD, LD-eS and LD-S states. Different letters indicate a significant difference between states (Newman–Keuls *post hoc* test following one-way ANOVA). For statistical significance, α was set at 0.05.

apoa1 and *sirt1* was increased consistently during the LD conditions, with mRNA levels in the order SD<LD-eS<LD-S state (P<0.05, Newman–Keuls *post hoc* test; Fig. 2G,H).

However, we found no difference in *adcyap1* ($F_{2,12}$=1.539, P=0.254) and *vps13a* ($F_{2,12}$=2.155, P=0.158; one-way ANOVA) expression, which were measured as markers of effects on migratory behaviour (Fig. 2I,J).

Protein expression

We assayed and compared MBH-specific proteome-wide changes between the LD-eS and LD-S states; exclusion of SD precluded any photoperiod effect. We identified a total of 503 proteins (Table S2). These enriched 27 functional pathways including the highly enriched carbon metabolism, TCA cycle, glycolysis and oxidative phosphorylation (Fig. 3A). A small number of proteins (28) were found to be differentially expressed between the LD-eS and LD-S states, with 21 upregulated and 7 downregulated proteins in the LD-S compared with the LD-eS state (Figs 3B, 4A). STRING network analysis revealed a mutual interaction of 11 out of the 28 differentially expressed proteins (Fig. 3B), and the enrichment of five functional pathways, namely astrocyte development (P=1.37E−04; PLP1, TSPAN2, VIM), regulation of neurotransmitter secretion (P=0.0160; SNCG, CAMK2A), glycolytic process (P=0.0337; PGAM1, GAPDH), intermediate filament protein (P=0.0460; VIM, NEFL) and PPAR signalling (P=0.0451; APOA1, FABP4) (Fig. 4B).

DISCUSSION

Photostimulated changes in gene expression

The present results show the molecular basis of FA biosynthesis and its transport in parallel with the photostimulated indices of the readiness for vernal migration in buntings. Here, we report elevated mRNA expression of *acc* and *dgat2* (*acc* mRNA levels in LD-S>SD, and *dgat2* mRNA levels in LD-S>SD and LD-eS) genes that code for ACC and DGAT2 enzymes involved in the hepatic FA biosynthesis pathway at the initial and final steps, respectively (Lu et al., 2015). At the same time, a similar *fasn* mRNA expression in all three states is inconsistent with the reported association of FASN enzyme activity with pre-migratory weight gain in buntings (Banerjee and Chaturvedi, 2016). Differences in *acc* and *fasn* gene expression in buntings might indicate their differential roles in lipogenesis: whereas *acc*-encoded ACC acts as the main rate-limiting enzyme and promotes lipogenesis at higher rates as required during the migratory state, the *fasn*-encoded FASN enzyme controls lipogenesis at a lower rate to fulfil short-term energy needs (Donaldson, 1979).

Changes in the hepatic *apoa1* and muscular *cd36* and *fabp3* paralleled the *acc* and *dgat2* mRNA levels, suggesting protein-mediated transport of FAs to the flight muscles, concurrently with their synthesis in the liver in the migratory state. FABP levels were also found to be elevated in the migratory state of western sandpipers (*Calidris mauri*; Guglielmo et al., 2002), white-throated sparrows (McFarlan et al., 2009) and blackheaded buntings (Srivastava et al., 2014). Elevated *cpt1* mRNA levels in flight muscles further support increased FA supply in the LD-S state. We suggest that the rate-limiting CPT1 enzyme mediates the mitochondrial uptake and β-oxidation of fatty acids (Shriver and Manchester, 2011) in ‘working’ muscles to meet energy demands of the migratory state in buntings.

We associate changes in gene expressions in MBH with activation (or inhibition) of hypothalamic molecular switches controlling the photoperiodic induction of the seasonal spring migration and gonadal maturation. For example, augmented Ca^{2+} transport, as indicated by upregulated *camk2a*, *camk1* and *atp2a2* expression, could be indicative of the overall alteration in neural processes, including the neurogenesis and maintenance of synaptic connections in the LD-S state (Berridge et al., 2000; Bouron, 2020; Boss et al., 2016). Although it is purely speculative at this time, we associate upregulated Ca^{2+} transport with enhanced neurogenesis and high neuronal activity in the MBH in order to integrate different sensory inputs and use the acquired information for navigation (Åkesson and Hedenström, 2007; Muheim et al., 2006; Warren et al., 2010). Interestingly, *camk2a* and *camk1* showed increased expression in LD-eS and LD-S, respectively, whereas *atp2a2* mRNA levels were elevated in both LD-eS and LD-S states. This might mean differential activation of molecular gears (enzymes) of the Ca^{2+}-signalling and transport cascade. Whereas calcium/calmodulin-dependent kinases were activated at different times, the ATPase sarcoplasmic Ca^{2+} transporting protein was activated consistently during the LD exposure. Elevated *atp2a2* mRNA levels were also found in photostimulated migratory blackheaded buntings (Sharma et al., 2018b). Perhaps, calcium also plays a role in switching on the necessary genomic changes (Bading, 2013) with the photostimulated transition from the non-migratory to migratory state in avian migrants. However, we would like to emphasize that the suggested Ca^{2+}-signalling and transport pathway does not preclude the involvement of alternative pathways including the release of hunger hormones, PPAR signalling, etc., in the photoperiodic induction of seasonal responses in migratory birds.

We also found change in *hspa8* and *sod1* gene expression, suggesting concurrent effects on physiological processes that include cellular stress and energy homeostasis in the MBH (Jones et al., 2008; Raja-Aho et al., 2012; Sharma et al., 2018b; Sharma and Kumar, 2019). We interpret that *hspa8*-encoded ATP-dependent molecular chaperones play a role in the protein quality check, and regulate protein transport and sorting via de-assembly of clathrin-coated vesicles (Stricher et al., 2013). Similarly, the enhanced *sod1* mRNA levels in the LD-S state are consistent with SOD1 playing a protective role against free superoxide radicals, which are probably produced in larger amounts during the photostimulated state. At the same time, the lack of change in *nos2* mRNA levels could be a neuroprotective response, as a prolonged cellular stress as might happen during the photostimulated migratory state could eventually increase nitric oxide, as well as nitric oxide-dependent post-translational redox modifications such as S-nitrosylations (SNO), which may interfere with neuronal functions and longevity (Valek et al., 2019). However, we caution that further experiments may be necessary to identify many more candidate molecules that constitute the multifaceted oxidative stress pathway system.

Further, changes in *apoa1* and *sirt1* expression are consistent with the idea of the involvement of a periphery–central feedback molecular circuit in the metabolic regulation (Cakir et al., 2009). We suggest that the MBH actively assesses the nutritional status and integrates appropriate responses at the whole-body level in order to respond to energy needs of the migratory state. Consistent with this, elevated *apoa1* and *sirt1* expression was found in the brain of northern wheatears and blackheaded buntings, respectively, when they were photostimulated and accumulated fat stores under stimulatory long days (Trivedi et al., 2014; Frias-Soler et al., 2020). This suggests the importance of *apoa1*-encoded ApoA1 (a major cholesterol transporter protein) in the photoperiodic induction of the migratory phenotype (Frias-Soler et al., 2020), although possible mechanisms remain unclear. Likewise, we

Journal of Experimental Biology (2021) 224, jeb242153. doi:10.1242/jeb.242153

LC MS/MS: hypothalamic protein expression
(annotated: 503; differentially expressed: 28)

A Enriched pathways

No.	Pathway	Gene no.
i	Carbon metabolism	43
ii	Oxidative phosphorylation	31
iii	Endocytosis	25
iv	Biosynthesis of amino acids	23
v	Glycolysis/gluconeogenesis	23
vi	Calcium signalling pathway	21
vii	Citrate cycle (TCA cycle)	20
viii	Phagosome	20
ix	Pyruvate metabolism	17
x	Adrenergic signalling in cardiomyocytes	17
xi	Gap junction	15
xii	Valine, leucine & isoleucine degradation	12
xiii	Propanoate metabolism	9
xiv	VEGF signalling pathway	9
xv	Butanoate metabolism	8
xvi	Pentose phosphate pathway	8
xvii	2-Oxocarboxylic acid metabolism	8
xviii	Arginine & proline metabolism	8
xix	Alanine, aspartate & glutamate metabolism	8
xx	Tryptophan metabolism	8
xxi	Glyoxylate & dicarboxylate metabolism	7
xxii	β-Alanine metabolism	7
xxiii	Lysine degradation	7
xxiv	Fatty acid degradation	7
xxv	Cysteine & methionine metabolism	7
xxvi	Arginine biosynthesis	5
xxvii	Vitamin B6 metabolism	3

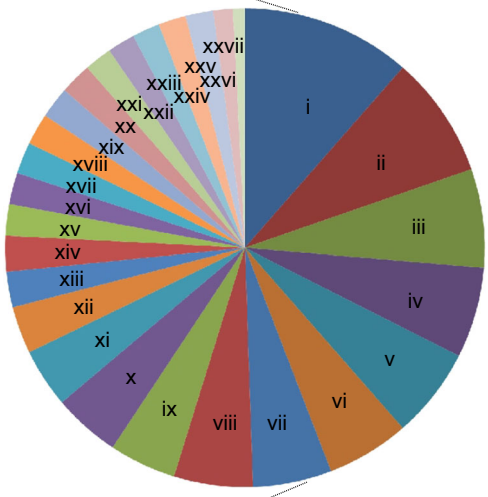

B Differentially expressed

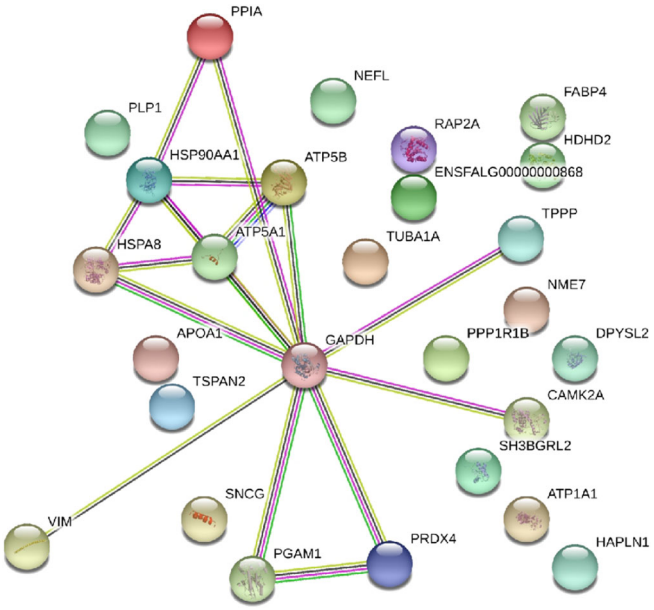

STRING network analysis: confidence value		
Node1	Node2	Score
VIM	GAPDH	0.43
TPPP	GAPDH	0.86
PRDX4	PGAM1	0.41
PRDX4	GAPDH	0.54
PPIA	HSP90AA1	0.43
PPIA	GAPDH	0.45
PGAM1	GAPDH	0.92
HSPA8	HSP90AA1	0.89
HSPA8	GAPDH	0.74
HSPA8	ATP5A1	0.51
HSP90AA1	GAPDH	0.65
HSP90AA1	ATP5B	0.73
HSP90AA1	ATP5A1	0.67
GAPDH	CAMK2A	0.50
GAPDH	ATP5B	0.68
GAPDH	ATP5A1	0.56
ATP5B	ATP5A1	0.99

Fig. 3. Proteome-wide changes in the mediobasal hypothalamus (MBH). (A) Pie chart showing 503 annotated proteins categorized into 27 functional pathways (tabulated on the left). (B) The STRING network of 28 differentially expressed proteins (LD-eS versus LD-S). The circles/nodes (proteins) and lines/edges (protein–protein interactions) are based on experimental evidence (edge colour: pink), gene neighbourhood (green), text mining (yellow), co-expression (black), databases (sky blue) and co-occurrence (blue). Empty nodes represent proteins with unknown 3D structure, while filled nodes represent proteins for which the 3D structure is known or predicted. The minimum required interaction score for the network was set to the medium confidence of 0.400.

suggest the role of *sirt1* in the regulation of appetite and metabolism, which are key components of the migratory state, based on evidence from mammals (Yamamoto and Takahashi, 2018). SIRT1 overexpression in pro-opiomelanocortin (POMC) neurons enhances energy expenditure, and its overexpression in agouti-related protein (AgRP) neurons suppresses food intake; this further suggests the neuron-specific role of SIRT1 in energy homeostasis (Yamamoto and Takahashi, 2018).

The lack of change in *adcyap1* and *vps13a* expression reinforces the view that they are not part of the hypothalamic gene switches

Journal of Experimental Biology (2021) 224, jeb242153. doi:10.1242/jeb.242153

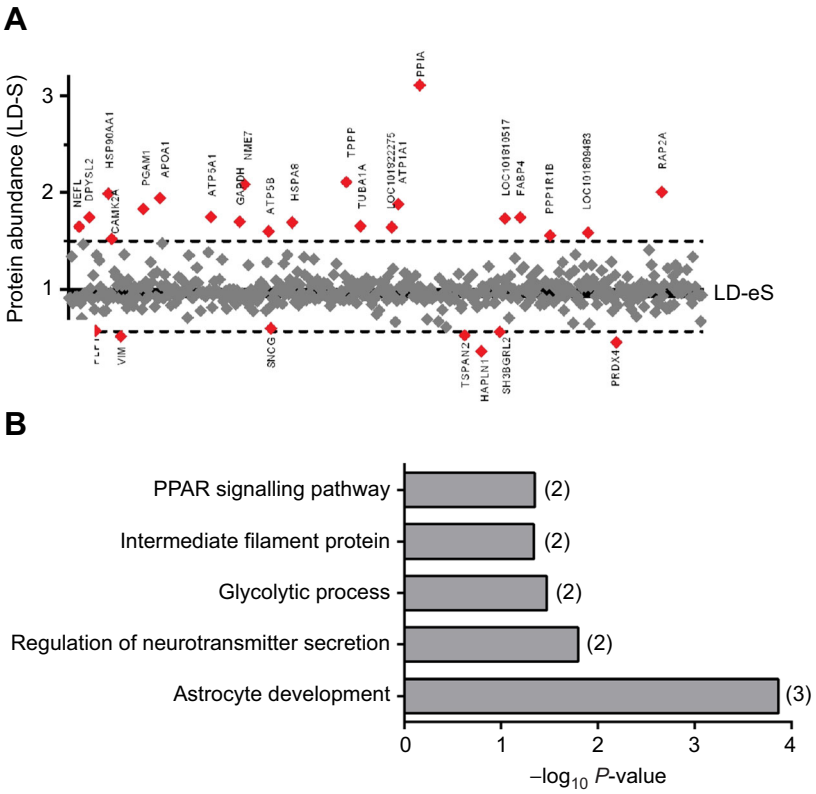

Fig. 4. Differentially expressed proteins in the MBH. (A) Protein abundance of differentially expressed proteins (red) in the LD-S relative to the LD-eS state (grey). (B) Proteins that enriched specific physiological pathways. Numbers in parentheses represent the number of proteins that enriched the pathway.

that are involved in the photoperiodic induction of the spring migratory phenotype. This is not surprising as this study did not test the migratory behaviour per se. Notably, variation in the allele size of *adcyap1*, not its expression level, was related to the intensity of Zugunruhe in European blackcaps (birds with longer *adcyap1* alleles displayed higher Zugunruhe; Mueller et al., 2011), but not in migratory juncos (*Junco hyemalis*; Peterson et al., 2013). Similarly, the association of *vps13a* expression was reported to relate to the migration directionality, not migratory state, of genetically closely related golden-winged warblers (*Vermivora chrysoptera*) and blue-winged warblers (*Vermivora cyanoptera*) migrating to winter in Central and South America, respectively (Toews et al., 2019). However, we will not completely discount an indirect role of the *adcyap1* gene, via its role as a light-sensitive molecule in circadian clock effects (Nagy and Csernus, 2007). The circadian clock regulates the phase transition in daily activity behaviour, when diurnal songbirds become predominantly night active with the onset of the migratory state (Bartell and Gwinner, 2005; Rani et al., 2006). Both *adcyap1* and *vps13a* could still be among candidate molecules of a 'migratory gene package' that via epistatic interactions determines/modifies the migration-associated behaviour and physiology in songbirds (Liedvogel et al., 2011).

MBH proteome: enriched pathways and differentially expressed proteins

The 503 annotated proteins were clustered in 27 physiological pathways, indicating a large coverage of the functional hypothalamus proteins by LC/MS-MS. The 28 differentially expressed proteins support the overall gene expression results on the role of Ca^{2+} signalling and transport, cellular stress and metabolic status, and protein-mediated transport of FA in the LD-S state. For example, higher CAMK2A protein levels suggest an activated calcium signalling pathway, perhaps for neuroadaptation in the migratory state. Similarly, low PRDX4 levels are consistent with high *sod1* and unchanged *nos2* mRNA levels in the LD-S state, suggesting an overall modulation of the anti-oxidant defence system at the MBH level (Schulte, 2011). Likewise, the downregulated PLP1 (proteolipid protein) and TSPAN2 (tetraspanin-2) of axon development and astrocyte development pathways probably played an activational role in shaping of the neural processes in the LD-S state. Although unknown in birds, single PLP or TSPAN2 knockout showed moderate, while double (PLP and TSPAN2) knockouts showed an enhanced activation of the astrocytes in mice (de Monasterio-Schrader et al., 2013).

There were significant protein-level changes, suggesting both re-modelling and transport of proteins at the cellular level, as might be required for an enhanced metabolic homeostasis in the LD-S state. In particular, we found upregulated expression of alpha and beta subunits of ATP-synthase (ATP5A1 and ATP5B), indicating enhanced ATP synthesis, and increased synthesis of ATP-dependent molecular chaperone HSPA8 and HSP90AA1 regulating protein transport (Stricher et al., 2013), PPIA involved in protein folding, and NME7 responsible for *de novo* formation of the microtubules (Liu et al., 2014). Upregulated TUBA1A, NEFL and TPPP, and concurrently downregulated VIM (vimentin) and SNCG (gamma-synuclein) proteins, further suggest cytoskeleton-dependent cellular remodelling of the proteins in the LD-S state. A similar differential hypothalamic cytoskeletal protein expression has been found between non-migratory and migratory states in Swainson's thrushes (*Catharus ustulatus*; Johnston et al., 2016). It may be noted that in Swainson's thrushes the characterization of both migratory and non-migratory states was based on fat accumulation and night activity, similar to that in the present bunting study.

We further propose that peripheral fat accumulation may serve as a physiological predictor of the vernal migratory state. Upregulated APOA1 and FABP4, which are FA transport proteins and enrich the

PPAR signalling pathway, may allow easy FA access through the blood–brain barrier either by passive diffusion or by using the ATP-dependent transporter proteins in the LD-S state (Tracey et al., 2018). This remains purely speculative at this time, however. Also, high GAPDH and PGAM1 protein levels, which catalyse the reversible steps of the glycolysis/gluconeogenesis metabolic pathway, suggest the overall increase of cellular metabolism in buntings; this can be important for flight-associated aerobic exercise in the migratory state.

In this first MBH-specific proteome-wide study of a migratory songbird, we have identified a subset of hypothalamic proteins that are potentially important and differentially expressed between LD-eS and LD-S states, as could be predicted from the gene expression results. In photostimulated buntings, we show that changes in the expression of cytoskeletal proteins and of those associated with astrocyte and axon development and PPAR signalling paralleled with the photostimulated migratory phenotype and testis maturation. These important results fill some gaps in our understanding of how the peripheral accumulation of fat could possibly serve as a physiological predictor of the migratory preparedness and readiness for vernal migration in obligate migratory songbirds.

A key question is what all the suggested mechanistic relationships based on molecular changes in the MBH mean for the physiology and/or ecology of a migratory bird. Although, the current study was not designed to answer this, we would argue that the activation (or inhibition) of molecular switches controlling the photoperiodic induction of migratory phenotype reinforces the view that hypothalamic substrates act as key integrators of the cascade of mechanisms that govern anticipatory energy intake in migrants in order to prepare them physiologically, so that they begin flying in time and arrive at their destination when conditions are most favourable. It may be noted further that the present molecular changes could account for the effects on metabolic processes that are linked to both the migratory and reproductive phenotypes, as captive buntings show body fattening and weight gain, as well as testis maturation when they are exposed to stimulatory LD conditions. This seems to have relevance to the overall ecology of avian migration, as the success of migration depends on the appropriate timing across multiple physiological systems that govern various sub-cycles of the annual life history, such as moult and reproduction, of a migratory species.

Finally, we show a series of molecular changes that include various physiological and metabolic pathways, but how these molecular pathways have functional connectivity and coordinate migration in songbirds remains unclear. This requires further study, perhaps in a field setting, to better address on the molecular mechanism(s) controlling the development of seasonal migration in avian migrants.

Acknowledgements
We thank Dr Pawan Malhotra, International Centre for Genetic Engineering and Biotechnology, New Delhi, India, for the help with quantitative proteomics.

Competing interests
The authors declare no competing or financial interests.

Author contributions
Conceptualization: V.K.; Methodology: A.S., D.S., P.G., I.K., V.K.; Validation: A.S.; Formal analysis: A.S., S.K.B., V.K.; Investigation: A.S., D.S., P.G., S.K.B., I.K.; Resources: S.K.B.; Data curation: A.S., V.K.; Writing - original draft: A.S., V.K.; Writing - review & editing: A.S., V.K.; Visualization: A.S., V.K.; Supervision: V.K.; Project administration: V.K.; Funding acquisition: V.K.

Funding
This study was supported by the Department of Biotechnology, New Delhi (Department of Biotechnology, Ministry of Science and Technology, India), through a major research grant (BT/PR4984/MED/30/752/2012) to V.K. A.S. received a research fellowship from Council of Scientific and Industrial Research, New Delhi.

Data availability
The mRNA sequences with their partial CDS can be accessed from GenBank (for accession numbers, see Table S1).

References
Åkesson, S. and Hedenström, A. (2007). How migrants get there: migratory performance and orientation. *Biosci.* **57**, 123-133. doi:10.1641/B570207
Ali, S. and Ripley, S. D. (1999). *Handbooks of the birds of India and Pakistan*, vol. 11. Bombay/London/New York: Oxford University Press.
Bading, H. (2013). Nuclear calcium signalling in the regulation of brain function. *Nat. Rev. Neurosci.* **14**, 593-608. doi:10.1038/nrn3531
Bairlein, F. (1985). Body weights and fat deposition of Palearctic passerine migrants in the Central Sahara. *Oecologia* **66**, 141-146. doi:10.1007/BF00378566
Banerjee, S. and Chaturvedi, C. M. (2016). Migratory prepration associated alterations in pectorals muscle biochemistry and proteome in Palearctic-Indian emberized migratory finch, red-headed bunting, *Emberiza bruniceps*. *Comp. Biochem. Physiol. D.* **17**, 9-25.
Barkan, S., Yom-Tov, Y. and Barnea, A. (2014). A possible relation between new neuronal recruitment and migratory behaviour in *Acrocephalus* Warblers. *Dev. Neurobiol.* **74**, 1194-1209. doi:10.1002/dneu.22198
Bartell, P. A. and Gwinner, E. (2005). A separate circadian oscillator controls nocturnal migratory restlessness in the songbird *Sylvia borin*. *J. Biol. Rhythms* **20**, 538-549. doi:10.1177/0748730405281826
Berridge, M. J., Lipp, P. and Bootman, M. D. (2000). The versality and universality of calcium signaling. *Nat. Rev. Mol. Cell Biol.* **1**, 11-21. doi:10.1038/35036035
Berthold, P. and Querner, U. (1988). Was Zugunruhe wirklich ist — eine quantitative Bestimmung mit Hilfe von VideoAufnahmen bei Infrarotlichtbeleuchtung. *J. Ornithol.* **129**, 372-375. doi:10.1007/BF01643380
Biebach, H. l., Friedrich, W. L. and Heine, C. (1986). Interaction of body mass, fat, foraging and stopover period in trans-Sahara migrating passerine birds. *Oecologia* **69**, 370-379. doi:10.1007/BF00377059
Boss, J., Liedvogel, M., Lundberg, M., Olsson, P., Reischke, N., Naurin, S., Åkesson, S., Hasselquist, D., Wright, A., Grahn, M. et al. (2016). Gene expression in the brain of a migratory songbird during breeding and migration. *Mov. Ecol.* **4**, 4. doi:10.1186/s40462-016-0069-6
Bouron, A. (2020). Transcriptomic profiling of Ca^{2+} transport system during the formation of the cerebral cortex in mice. *Cells* **9**, 1800. doi:10.3390/cells9081800
Budki, P., Rani, S., Kumar, V. (2009). Food deprivation during photosensitive and photorefractory life history stages affects reproductive cycle in the migratory redheaded bunting (*Emberiza bruniceps*). *J. Exp. Biol.* **212**, 225-230. doi:10.1242/jeb.024190
Bustin, S. A., Benes, V., Garson, J. A., Hellemans, J., Huggett, J., Kubista, M., Mueller, R., Nolan, T., Pfaffl, M. W., Shipley, G. L. et al. (2009). The MIQE guidelines: minimum Information for publication of quantitative real-time PCR experiments. *Clinical Chem.* **55**, 611-622. doi:10.1373/clinchem.2008.112797
Çakir, I., Perello, M., Lansari, O., Messier, N. J., Vaslet, C. A. and Nillni, E. A. (2009). Hypothalamic sirt1 regulates food intake in a rodent model system. *PLoS One* **4**, e8322. doi:10.1371/journal.pone.0008322
Cassone, V. M. and Yoshimura, T. (2015). Circannual cycles and photoperiodism. In *Sturkie's Avian Physiology* (ed. C. G. Scanes), pp. 829-844. New York: Springer-Verlag.
de Monasterio-Schrader, P., Patzig, J., Möbius, W., Barrette, B., Wagner, T. L., Kusch, K., Edgar, J. M., Brophy, P. J. and Werner, H. B. (2013). Uncoupling of neuroinflammation from axonal degeneration in mice lacking the myelin protein tetraspanin-2. *Glia* **61**, 1832-1847. doi:10.1002/glia.22561
Dennis, G., Sherman, B. T., Hosack, D. A., Yang, J., Gao, W., Lane, H. C. and Lempicki, R. A. (2003). DAVID: database for annotation, visualization, and integrated discovery. *Genome Biol.* **4**, R60. doi:10.1186/gb-2003-4-9-r60
Donaldson, W. E. (1979). Regulation of fatty acid synthesis. *Fed. Proc.* **38**, 2617-2621.
Frias-Soler, R. C., Pildaín, L. V., Pârâu, L. G., Wink, M. and Bairlein, F. (2020). Transcriptome signatures in the brain of a migratory songbird. *Comp. Biochem. Physiol. D* **34**, 100681.
Fusani, L., Coccon, F., Mora, A. R. and Goymann, W. (2013). Melatonin reduces migratory restlessness in Sylvia warblers during autumnal migration. *Front. Zool.* **10**, 79. doi:10.1186/1742-9994-10-79
Gong, X., Tao, R. and Li, Z. (2006). Quantification of RNA damage by reverse transcription polymerase chain reaction. *Analytical Biochem.* **357**, 58-67. doi:10.1016/j.ab.2006.06.025
Guglielmo, C. G., Haunerland, N. H., Hochachka, P. W. and Williams, T. D. (2002). Seasonal dynamics of flight muscle fatty acid binding protein and catabolic enzymes in a migratory shorebird. *Am. J. Physiol.* **282**, R1405-R1413.
Gwinner, E. (1972). Adaptive functions of circannual rhythms in warblers. *Proc. Int. Ornitol. Congr.* **15**, 218-236.
Harrington, M. E., Hoque, S., Hall, A., Golombek, D. and Biello, S. (1999). Pituitary adenylate cyclase activating peptide phase shifts circadian rhythms in a

manner similar to light. *J. Neurosci.* **19**, 6637-6642. doi:10.1523/JNEUROSCI.19-15-06637.1999
Helms, C. W. and Drury, W. H. (1960). Winter and migratory weight and fat: Field studies on some North-American buntings. *Bird-Banding* **31**, 1-40. doi:10.2307/4510793
Johnston, R. A., Paxton, K. L., Moore, F. R., Wayne, R. K. and Smith, T. B. (2016). Seasonal gene expression in a migratory songbird. *Mol. Ecol.* **25**, 5680-5691. doi:10.1111/mec.13879
Jones, S., Pfister-Genskow, M., Cirelli, C. and Benca, R. M. (2008). Changes in brain gene expression during migration in the white-crowned sparrow. *Brain Res. Bull.* **76**, 536-544. doi:10.1016/j.brainresbull.2008.03.008
Kumar, V. and Mishra, I. (2018). Circannual rhythms. In *Encyclopedia of Reproduction* (ed. M. K. Skinner), pp. 442-450. Academic Press, Elsevier.
LaDage, L. D., Roth, T. C. and Pravosudov, V. V. (2011). Hippocampal neurogenesis is associated with migratory behaviour in adult but not juvenile sparrows (*Zonotrichia leucophrys* ssp.). *Proc. R. Soc. B: Biol. Sci. B* **278**, 138-143. doi:10.1098/rspb.2010.0861
Liedvogel, M., Åkesson, S. and Bensch, S. (2011). The genetics of migration on the move. *Trends Ecol. Evol.* **26**, 561-569. doi:10.1016/j.tree.2011.07.009
Liu, P., Choi, Y.-K. and Qi, R. Z. (2014). NME7 is a functional component of the γ-tubulin ring complex. *Mol. Biol. Cell* **25**, 2017-2025. doi:10.1091/mbc.e13-06-0339
Livak, K. J. and Schmittgen, T. D. (2001). Analysis of relative gene expression data using real-time quantitative PCR and the $2^{-\Delta\Delta CT}$ Method. *Methods* **25**, 402-408. doi:10.1006/meth.2001.1262
Lofts, B. (1975). Environmental control of reproduction. *Symp. Zooo. Soc.* **25**, 177-197.
Lu, L., Chen, Y., Wang, Z., Li, X., Chen, W., Tao, Z., Shen, J., Tian, Y., Wang, D., Li, G. et al. (2015). The goose genome sequence leads to insights into the evolution of waterfowl and susceptibility to fatty liver. *Genome Biol.* **16**, 89. doi:10.1186/s13059-015-0652-y
Lupi, S., Goymann, W., Cardinale, M. and Fusani, L. (2016). Physiological conditions influence stopover behaviour of short-distance migratory passerines. *J. Ornithol.* **157**, 583-589. doi:10.1007/s10336-015-1303-5
Majumdar, G., Rani, S. and Kumar, V. (2015). Hypothalamic gene switches control transitions between seasonal life history states in a nightmigratory photoperiodic songbird. *Mol. Cell. Endocrinol.* **399**, 110-121. doi:10.1016/j.mce.2014.09.020
Malik, S., Rani, S. and Kumar, V. (2009). Wavelength dependency of light induced effects on photoperiodic clock in the migratory blackheaded bunting (*Emberiza melanocephala*). *Chronobiology Int.* **21**, 367-384. doi:10.1081/CBI-120038742
McFarlan, J. T., Bonen, A. and Guglielmo, C. G. (2009). Seasonal upregulation of protein mediated fatty acid transport in flight muscles of migratory white-throated sparrows (*Zonotrichia albicollis*). *J. Exp. Biol.* **212**, 2934-2940. doi:10.1242/jeb.031682
Mishra, I., Singh, D. and Kumar, V. (2018). Temporal expression of c-fos and genes coding for neuropeptides and enzymes of amino acid and amine neurotransmitter biosynthesis in retina, pineal and hypothalamus of a migratory songbird: evidence for circadian rhythm dependent seasonal responses. *Neuroscience* **371**, 309-324. doi:10.1016/j.neuroscience.2017.12.016
Mueller, J. C., Pulido, F. and Kempenaers, B. (2011). Identification of a gene associated with avian migratory behaviour. *Proc. Royal Soc. B.* **278**, 2848-2856. doi:10.1098/rspb.2010.2567
Muheim, R., Phillips, J. B. and Åkesson, S. (2006). Polarized light cues underlie compass calibration in migratory songbirds. *Science* **313**, 837-839.
Nagy, A. D. and Csernus, V. J. (2007). The role of PACAP in the control of circadian expression of clock genes in the chicken pineal gland. *Peptides* **28**, 1767-1774. doi:10.1016/j.peptides.2007.07.013
Nakao, N., Ono, H., Yamamura, T., Anraku, T., Takagi, T., Higashi, K., Yasuo, S., Katou, Y., Kageyama, S., Uno, Y. et al. (2008). Thyrotrophin in the pars tuberalis triggers photoperiodic response. *Nature* **452**, 317-322. doi:10.1038/nature06738
Newton, I. (2008). *The migration ecology of birds*. London, UK: Academic Press.
Nowak, J. Z. and Zawilska, J. B. (2003). PACAP in Avians: origin, occurrence, and receptors – pharmacological and functional considerations. *Curr. Pharm. Des.* **9**, 467-481. doi:10.2174/1381612033391586
Odum, E. P. (1960). Lipid deposition in nocturnal migrant birds. *Proc. Int. Ornitol. Congr.* 563-576.
Olkowicz, S., Kocourek, M., Lučan, R. K., Porteš, M., Fitch, W. T., Herculano-Houzel, S. and Němec, P. (2016). Birds have primate-like numbers of neurons in the forebrain. *Proc. Nat. Acad. Sci. USA* **113**, 7255-7260. doi:10.1073/pnas.1517131113
Peterson, M. P., Abolins-Abols, M., Atwell, J. W., Rice, R. J., Milá, B. and Ketterson, E. D. (2013). Variation in candidate genes CLOCK and ADCYPA1 does not consistently predict differences in migratory behaviour in the songbird genus *Junco*. *F1000Research* **2**, 115. doi:10.12688/f1000research.2-115.v1
Raja-Aho, S., Kanerva, M., Eeva, T., Lehikoinen, E., Suorsa, P., Gao, K., Vosloo, D. and Nikinmaa, M. (2012). Seasonal variation in the regulation of redox state and some biotransformation enzyme activities in the barn swallow (*Hirundo rustica L.*). *Physiol. Biochem. Zool.* **85**, 148-158. doi:10.1086/664826
Ramenofsky, M. (1990). Fat storage and fat metabolism in relation to migration. In *Bird Migration: Physiology and Ecophysiology* (ed. E. Gwinner), pp. 214-231. New York: Springer-Verlag.
Ramenofsky, M. and Wingfield, J. C. (2007). Regulation of migration. *Biosciences* **57**, 135-143. doi:10.1641/B570208
Rani, S., Malik, S., Trivedi, A. K., Singh, S. and Kumar, V. (2006). A circadian clock regulates migratory restlessness in the blackheaded bunting, *Emberiza melanocephala*. *Curr. Sci.* **91**, 1093-1096.
Rani, S., Singh, S., Malik, S. and Kumar, V. (2017). Insights into the regulation of spring migration in songbirds. In *Biological Timekeeping: Clcoks, Rhythms and Behaviour* (ed. V. Kumar), pp. 625-642. New Delhi: Springer Nature (Springer India).
Rastogi, A., Kumari, Y., Rani, S. and Kumar, V. (2011). Phase inversion of neural activity in the olfactory and visual systems of a night-migratory bird during migration. *European J. Neurosci.* **34**, 99-109. doi:10.1111/j.1460-9568.2011.07737.x
Rastogi, A., Kumari, Y., Rani, S. and Kumar, V. (2013). Neural correlates of migration: activation of hypothalamic clock(s) in and out of migratory state in the blackheaded bunting (*Emberiza melanocephala*). *PLoS One* **8**, e70065. doi:10.1371/journal.pone.0070065
Schulte, J. (2011). Peroxiredoxin 4: a multifunctional biomarker worthy of further exploration. *BMC Med.* **9**, 137. doi:10.1186/1741-7015-9-137
Sharma, A. and Kumar, V. (2019). Metabolic plasticity mediates differential responses to spring and autumn migrations: evidence from gene expression patterns in migratory buntings. *Exp. Physiol.* **104**, 1841-1857. doi:10.1113/EP087974
Sharma, A., Singh, D., Malik, S., Gupta, N. J., Rani, S. and Kumar, V. (2018a). Difference in control between spring and autumn migration in birds: insights from seasonal changes in hypothalamic gene expression in captive buntings. *Proc. Royal Soc. B* **285**, 20181531. doi:10.1098/rspb.2018.1531
Sharma, A., Singh, D., Das, S. and Kumar, V. (2018b). Hypothalamic and liver transcriptome from two crucial life history stages in a migratory songbird. *Exp. Physiol.* **103**, 559-569. doi:10.1113/EP086831
Sharp, P. J. (2005). Photoperiodic regulation of seasonal breeding in birds. *Ann. NY Acad. Sci.* **1040**, 189-199. doi:10.1196/annals.1327.024
Shriver, L. P. and Manchester, M. (2011). Inhibition of fatty acid metabolism ameliorates disease activity in an animal model of multiple sclerosis. *Sci. Rep.* **1**, 79. doi:10.1038/srep00079
Singh, D., Trivedi, A. K., Rani, S., Panda, S. and Kumar, V. (2015). Circadian timing in central and peripheral tissues in a migratory songbird: dependence on annual life-history states. *FASEB J.* **29**, 4248-4255. doi:10.1096/fj.15-275339
Srivastava, S., Rani, S. and Kumar, V. (2014). Photoperiodic induction of premigratory phenotype in a migratory songbird: Identification of metabolic proteins in flight muscles. *J. Comp. Physiol. B* **184**, 741-751. doi:10.1007/s00360-014-0827-y
Staib-Lasarzik, I., Kriego, O., Timaru-Kast, R., Pieter, D., Werner, C., Engelhard, K. and Thal, S. C. (2014). Anesthesia for euthanasia influences mRNA expression in healthy mice and after traumatic brain injury. *J. Neurotrauma* **31**, 1664-1671. doi:10.1089/neu.2013.3243
Stevenson, T. J. and Kumar, V. (2017). Neural control of daily and seasonal timing of songbird migration. *J. Comp. Physiol. A* **203**, 399-409. doi:10.1007/s00359-017-1193-5
Stricher, F., Macri, C., Ruff, M. and Muller, S. (2013). HSPA8/KSC70 chaperone protein structure, function, and chemical targeting. *Autophagy* **9**, 1937-1954. doi:10.4161/auto.26448
Sur, S., Sharma, A., Trivedi, A. K., Bhardwaj, S. K. and Kumar, V. (2019). Temperature affects liver and muscle metabolism in photostimulated migratory redheaded buntings (*Emberiza bruniceps*). *J. Comp. Physiol. B.* **189**, 623-635. doi:10.1007/s00360-019-01229-5
Sur, S., Sharma, A., Bhardwaj, S. K. and Kumar, V. (2020). Involvement of steroid and antioxidant pathways in spleen mediated immunity on migratory birds. *Comp. Biochem. Physiol. A* **250**, 110790. doi:10.1016/j.cbpa.2020.110790
Surbhi, and Kumar, V. (2014). Avian photoreceptors and their role in the regulation of daily and seasonal physiology. *Gen. Comp. Endocr.* **220**, 13-22.
Toews, D. P. L., Taylor, S. A., Streby, H. M., Kramer, G. R. and Lovette, I. J. (2019). Selection on VPS13A linked to migration in a songbird. *Proc. Nat. Acad. Sci. USA* **116**, 18272-18274. doi:10.1073/pnas.1909186116
Tracey, T. J., Steyn, F. J., Wolvetang, E. J. and Ngo, S. T. (2018). Neuronal lipid metabolism: multiple pathways driving functional outcomes in health and disease. *Front. Mol. Neurosci.* **11**, 10. doi:10.3389/fnmol.2018.00010
Trivedi, A. K., Kumar, J., Rani, S. and Kumar, V. (2014). Annual life history-dependent gene expression in the hypothalamus and liver of a migratory songbird: Insights into the molecular regulation of seasonal metabolism. *J. Biol. Rhythms* **29**, 332-345. doi:10.1177/0748730414549766
Valek, L., Heidler, J., Scheving, R., Witting, I. and Tegeder, I. (2019). Nitric oxide contributes to protein homeostasis by S-nitrosylations of the chaperone HSPA8 and the ubiquitin ligase UBE2D. *Redox Biol.* **20**, 217-235. doi:10.1016/j.redox.2018.10.002

Warren, W. C., Clayton, D. F., Ellegren, H., Arnold, A. P., Hillier, L. W., Künstner, A., Searle, S., White, S., Vilella, A. J., Fairley, S. et al. (2010). The genome of a songbird. *Nature* **464**, 757-762. doi:10.1038/nature08819

Weber, J.-M. (2009). The physiology of long distance migration: extending the limit of endurance metabolism. *J. Exp. Biol.* **212**, 593-597. doi:10.1242/jeb.015024

Wingfield, J. C. and Farner, D. S. (1978). The endocrinology of a naturally breeding population of the white-crowned sparrow (*Zonotrichia leucophrys pugetensis*). *Physiol. Zool.* **51**, 188-205. doi:10.1086/physzool.51.2.30157866

Yamamoto, M. and Takahashi, Y. (2018). The essential role of SIRT1 in hypothalamic-pituitary axis. *Front. Endocrinol.* **9**, 605. doi:10.3389/fendo.2018.00605

Yoshimura, T. (2006). Molecular mechanism of the photoperiodic response of gonads in birds and mammals. *Comp. Biochem. Physiol. A. Mol. Integr. Physiol.* **144**, 345-350. doi:10.1016/j.cbpa.2005.09.009

Yugandhan, K., Gupta, S. and Yu, H. (2019). Inferring protein-protein interaction networks from mass-spectrometry based approaches: A mini review. *Comput. Struct. Biotechnol.* **17**, 805-811. doi:10.1016/j.csbj.2019.05.007

Figure S1

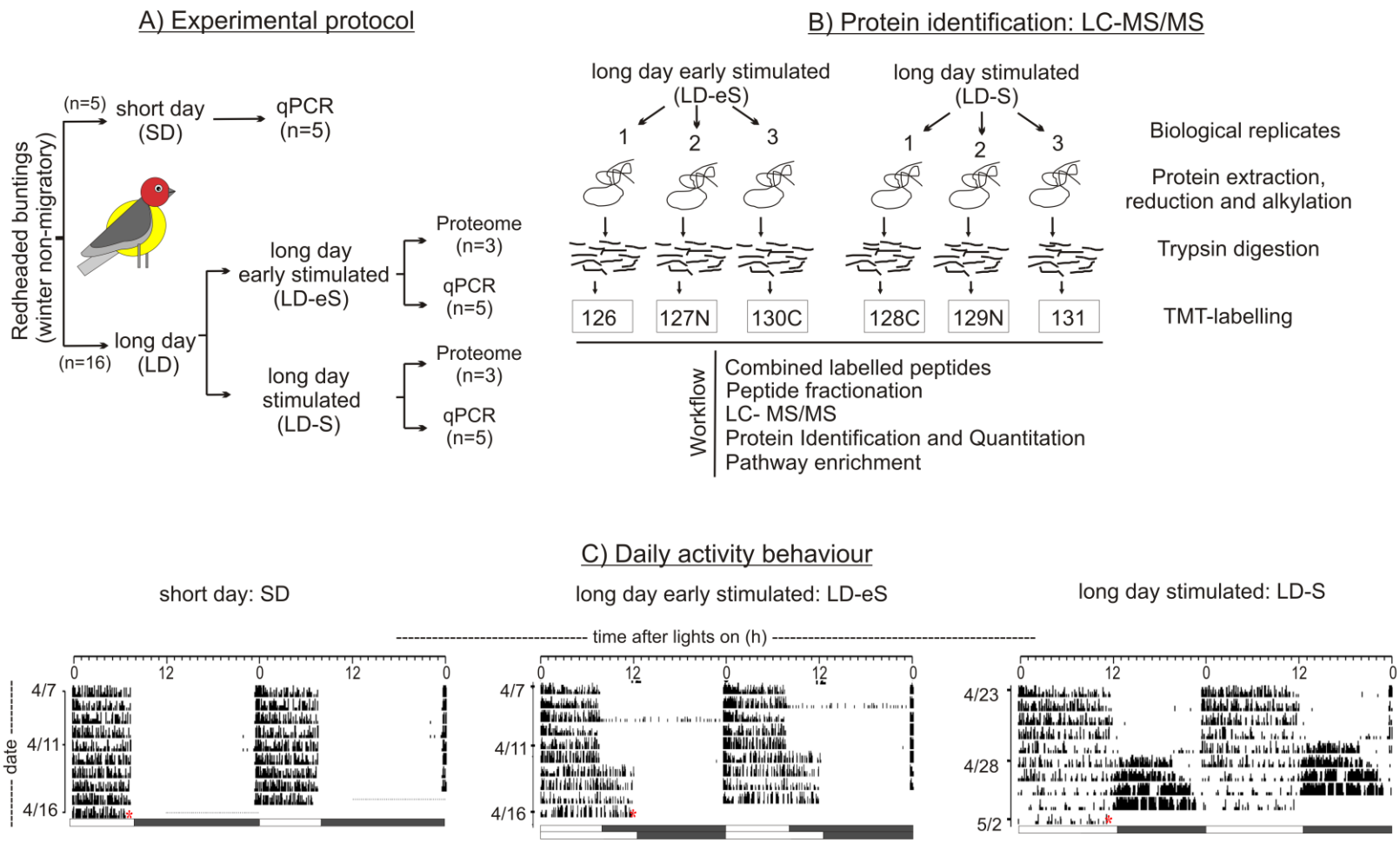

Figure S1: Top panel: Left - Photosensitive male redheaded buntings (n=21) were exposed to stimulatory long days (LD: 12.5L:11.5D; n=16) for four days (LD early stimulated, LD-eS; n = 8) or until they exhibited 4 nights of *Zugunruhe* (migratory restlessness, a reliable index of the migratory state, LD stimulated, LD-S n =8), with controls maintained on short days (8 h of light and 16 h of dark, 8L:16D; SD; n=5). Post-mortem, we performed gene expression assays in the liver, muscle and mediobasal hypothalamus (MBH; n = 5) and MBH-specific quantitative proteomics (n = 3), for which tissue samples were collected half an hour before the lights off (hour 7.5 for SD, hour 12 for LD; hour 0 = lights on). Note: Proteome assay was done for only LD-eS and LD-S states to preclude the photoperiod effect. Right - The procedure for the extraction, purification and identification of the proteins in LD-eS and LD-S states. Bottom panel: (C) Representative 24 h actograms of an individual birds each from SD, LD-eS and LD-S photoperiod-induced states. To give a better visual resolution of changes over 24 h, if any, in the activity-rest pattern of each individual is presented in a double raster-plot (actogram) in which the activity on successive days has been presented both sideways and underneath.

Table S1: Gene specific primers used for measurement of mRNA expression by q-PCR

Gene	Primer Sequence	Accession No.
ba	F: 5' TGTTACCCACACTGTGCCCATCTA 3' R: 5' TTCATGAGGTAGTCCGTCAGGTCA 3'	KC874663.1
acc	F: 5' TTCTACTTCCTGGAGCTGAACC 3' R: 5' TGATGTCCTTGATCCTGTGC 3'	KJ406210.1
fasn	F: 5' AAGAGGGTGTGTTCGCAAAG 3' R: 5' TGTACTGATCCATCGTGCTG 3'	KJ420917.1
dgat2	F: 5' TTTCTTTAGGCACGGGATCG 3' R: 5' AGCACAGAGATGATTTGGAGTT 3'	MF979806
apoa1	F: 5'AAGGAAGCCATTGCCCAGTT 3' R: 5' CACATCTCCCGCACCTCTTT 3'	MT974478
fabp3	F: 5' GCACCTTCAAGAACACCGAGATCAC 3' R: 5' GTCTCCTTCCCCTCCCACTTC 3'	MK014290
cd36	F: 5' TGGAAAGGCCACTGTGATATG 3' R: 5' GCAAATGTCCGAGGAGAAGAA 3'	MK014291
cpt1	F: 5' GCCCATCTAGCTGGCTTATT 3' R: 5' CAAGTGTTCTGTTGATCTTGGC 3'	MK747359
camk1	F: 5' CTACATCCTGCTCTGTGGTTAC 3' R: 5' GGTGAGTCAAACTCGTACTCTG 3'	MT974476
camk2a	F: 5' CCAGTTCCAGCGTTCAGTTA 3' R: 5' CGAAGTCGCCATTGCTTATTG 3'	MT974477
atp2a2	F: 5' GGAGACAAGGTTCTTGCTGATA 3' R:5' CAGGGTCCGTGTGCTTAAT 3'	MF777024
adcyap1	5' ACATAGACGGCATCTTCACG 3' 5' CAGGACGGCTGCTAAGTATTTC 3'	MF427847
vps13a	F: 5' GTGAATGGCAGTACACTTACGA 3' R: 5' TGGCATGGAAGACAGACTTAAC 3'	MT394488
sod1	F: 5' TGCGGAGTGATTGGGATTG 3' R: 5' CATCTGGAAGTTGCAGGAAGA 3'	MK868466
nos2	F: 5' ATGACCTTGCTGTTCGGATG 3' R: 5' AGTCTGGAGTAAGCTGTGTAGA 3'	MK868465
hspa8	F: 5' AGAGCTCAACAAGAGCATCAA 3' R: 5' GTCCTGCACGTTCTCAGAC 3'	MF777031
sirt1	5' GGAGTGCAAGAAGATCATGG 3' 5' TTGCTTGAGGATCTGGAAGG 3'	KJ420926.1

Table S2. Annotated hypothalamic proteins of redheaded buntings in long day early stimulated (LD-eS) and stimulated (LD-S) states.

Click here to Download Table S2